Application of GI-SAXS to Near-surface Microstructures in Al-based Alloys

Hiroshi Okuda, Shojiro Ochiai and Kazuki Ito*
International Innovation Center, Kyoto University, Yoshida Honmachi, Sakyo-ku Kyoto 606-8501 Japan
Fax: 81-75-753-4841, e-mail: okuda@iic.kyoto-u.ac.jp
*SSRL, Stanford University
Fax: 1-650-926-2258, e-mail: kazuki@slac.stanford.edu

Structure of binary Al-Ag and Al-Zn alloys near the sample surface has been examined by small-angle X-ray scattering with grazing incidence (GI-SAXS) utilizing synchrotron radiation. The alloys are well known to form Guinier-Preston (GP) zones of a couple of nanometers in size upon heat treatment. The transformation takes place with quenched-in vacancies. Depletion of quenched-in vacancies near the free surface and grain boundary eventually lead to a delay in diffusion near the region. By using GI-SAXS measurements with various angle of incidence, we evaluated the distribution of average zone size as a function of depth from the surface. The merit and the limitation of the present approach to examine precipitation structure near the surface have been discussed with a use of kinematical model calculations.

The microstructures obtained in the present analysis showed that the average size very close to the surface was about 23% smaller than the bulk average, and the average size changes within a submicron distance from the surface. Present result has been discussed from a viewpoint of kinetic theory of conventional precipitation-free zone formation.

Key words: Grazing-incidence small-angle scattering, Al alloys, Surface effect, Vacancy depletion

1. INTRODUCTION

In many age-hardenable aluminum alloys, metastable precipitates or GP zones form during annealing. These precipitates or zones are smaller, or sometimes even vanish near the sample surfaces and grain boundaries. These area without precipitates are called precipitation free zones (PFZ), and often deteriorate mechanical properties, in particular under cyclic loading. Therefore, the mechanism of PFZ formation and the way to control it have been of one of the major concern in microstructure control for practical Al based alloys[1-2]. Since the formation of Guinier-Preston (GP) zones is often controlled by quenched-in excess vacancies, one of the explanation of the mechanism of PFZ formation is the decrease in vacancy concentration near the surface, since the grain boundaries as well as free surfaces are the sink of quenched-in excess vacancies. Decrease in vacancy concentration leads to decrease in diffusivity, and the delay in precipitation process. Another explanation is a depletion of solute concentration due to segregation or heterogeneous precipitation at the grain boundaries and surfaces. The experimental results [1,2] suggest that PFZ may form under both conditions, it was hard to figure out the mechanism and the kinetics of such microstructure formation, since the both effects, namely the vacancy depletion and the solute depletion were often observed concomitantly. Therefore, it is worthwhile to inquire into the microstructure near the surface nondestructively, where no surface precipitation is expected.

In the present work, we examined the precipitation structure of Al-1.5at% Ag alloys near the surface by using Grazing-Incidence Small-Angle X-ray Scattering (GI-SAXS). GI-SAXS is quite attractive when we are interested in the microstructure very close to the surface, but not in the uppermost surface, which can be examined directly by a scanning probe microscopy.

Conventional small-angle scattering in transmission geometry is a rather well established method in the research of precipitation processes in metallic materials[3], and depending on the optics installed, we can measure the precipitates ranging from less than a nanometer to about a micrometer in radius without problem. On the other hand, GI-SAXS may suffer its specific limitation arising from the limit of the shade of the sample itself[4]. This limitation may be a problem under certain conditions, which we will discuss later.

From the viewpoint of the kinetics of phase transformation, we need some supplemental tool to examine how the microstructure may formed. In the present work, a kinetic Ising model using Kawasaki Dynamics is used to examine whether the microstructure is explained by the kinetics we assumed.

2. EXPERIMENTAL

We conducted grazing-incidence small-angle scattering experiment for aged single-crystalline Al-Ag binary alloy samples. Samples used were Al-1.5% Ag single crystalline plates of about 0.2 mm in thickness with (110) surfaces.

Samples were homogenized at 693 K for 1.8 ks, and quenched into iced water. Then after electrochemical polishing to obtain well-defined mirror surface, they are solution treated for 300 s and quenched into iced water again. Immediate after quenching, the samples were aged at 423 K for 60 ks to form GP zones.

GI-SAXS experiments were carried out at the beamline 15A of Photon Factory, a synchrotron

radiation facility in Tsukuba. The wavelength of the X-ray was 0.15nm. Figure 1 shows a schematic view of the present GI-SAXS measurements. A rotation stage was placed at the sample position, and the height of the sample surface was controlled with a translation stage on the rotation stage. Scattering intensities were measured by using a linear proportional detector (1d-PSPC).
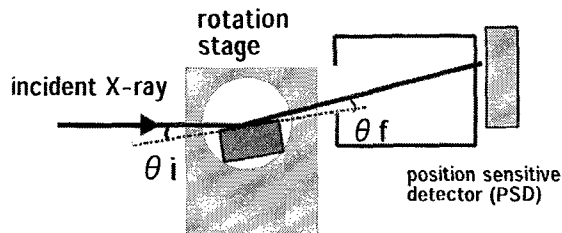
Fig.1   Schematic drawing of the present GI-SAXS experiments at Photon Factory.

3. SIMULATION PROCEDURE

A set of computer simulations using kinetic Ising model with Kawasaki dynamics were carried out to examine if the microstructure may form under the heat treatment conditions and the mechanism we assumed. A fcc model lattice with 60 x 60 x 300 unit cells was used, with the long side, x, corresponding to the direction normal to the surface, and the short sides, y and z, to the one parallel to the surface. Periodic boundary condition is used in y and z directions, whereas simple reflection condition was used for x direction.

The system was solution treated for a short period and then quenched into lower temperature for the first heat treatment up to about 10^3 MCS with a mobility distribution described by a error function, meaning that the vacancy depletion occurs near the surface. This heat treatment corresponds to the formation of GP zones during quench. Experimentally, it is well known that GP zones form during quench, and at low temperatures near room temperature, the phase separation proceeds mostly by the quenched-in excess vacancies in Al-based alloys. Then for the second annealing, we increase the temperature, with a uniform vacancy concentration. The temperature of the second heat-treatment in the experiments was high enough, and the kinetics of the phase separation of most Al-based alloys at the temperatures are explained with the equilibrium thermal vacancies. From the simulation, the evolution of cluster size was discussed.

4. RESULTS AND DISCUSSIONS
4.1 Guinier radius

The scattering intensities were normalized in terms of the exposure time and the incident X-ray intensity. After background subtraction, they were analyzed by the Guinier approximation. Figure 2 gives the Guinier plot of the intensity obtained for several angles of incidence. The plot for conventional transmission SAS for the same sample was also plotted in the figure.
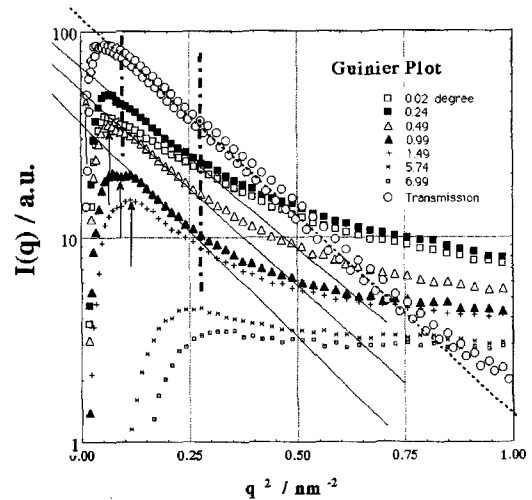
Fig. 2   Guinier plots of the intensities obtained for GI-SAXS and for conventional SAXS. It is noted that the range that Guinier approximation hold is much larger for conventional SAXS.

The slopes in the Guinier plot are similar for the transmission measurement and for GI-SAXS with the incident angle smaller than 1.5 degree. It is seen that the onset of Guinier region is slightly smaller for smaller angle of incidence, and at much larger angle of incidence with 5.76 degree, the information on the zone size is already lost due to a geometrical limitation that the shade of the sample itself hit the Guinier region, and lower bound is mostly determined the shade of the sample against air scattering at upper stream beam path. For the upper limit of the Guinier region, the transmission geometry gave much larger limit. This is not explained by a geometrical consideration. This smaller upper limit for GI-SAXS may be explained by the overlapping of surface roughness scattering, and could not be subtracted in the present measurement.

The Guinier radius obtained from the plot was shown as a function of the incident angle in Fig. 3.
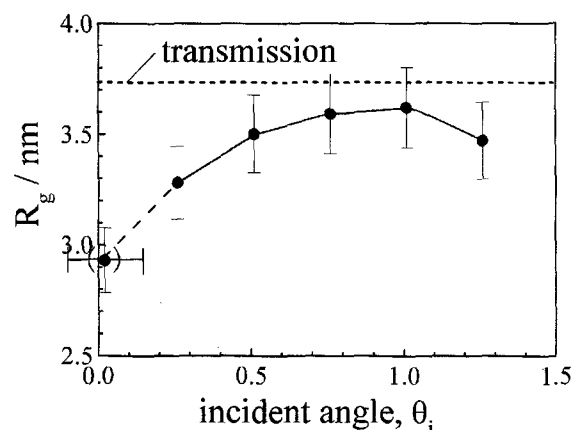
Fig. 3   The Guinier radius as a function of the angle of incidence, θi.

The Guinier radius for transmission geometry is the largest, and a peak in the radius is observed in the intermediate angle of about 0.7 degree. Although the error may be large due to the narrower range of Guinier region for GI-SAXS, figure 3 suggests that the average size of GP zone is depth dependent.

When the distribution of precipitates is spatially uniform, the GI-SAXS intensity is simply expressed as [4],

$$I(q) = T_i(\theta_i) \cdot T_f(\theta_f) S(q) \qquad (1)$$

where T's denote the Fresnel transmission coefficients for incoming and outgoing wave. However, we observed an angle-dependent Guinier radius. From what we know about the kinetics of GP zone formation, we may expect the microstructure of the sample as illustrated in Fig. 4.

surface
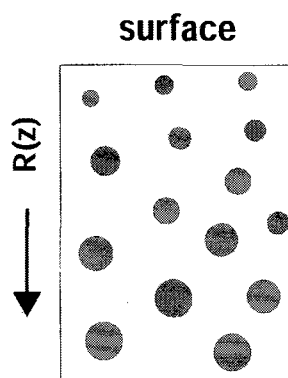
Fig.4 Schematic illustration of the microstructure in the sample. Vacancy depletion leads to a simple delay in the average GP zone size, and the average composition is uniform over the whole sample.

Since the microstructural change directly induced by vacancy depletion should be the spatial change in the time scale, we assumed that the composition is uniform along the surface normal (z) direction. This condition simplify the situation, since the Fresnel coefficient is dependent on the average composition, so that we can treat the sample as a uniform material as far as the refractive index is concerned. In order to consider the change of the average radius in the z direction, we adopted a simple kinematical approach. When the Guinier radius at the depth z is denoted by Rg(z), we may write down the intensity as;

$$I(q) = \int_0^\infty I(q,z) \exp(-\mu z / \sin\theta_i)$$

$$* \exp(-\mu z / \sin\theta_f) dz \qquad (2)$$

The intensity from the slice z dz may be approximated by taking the Guinier approximation and the constant volume fraction into account as ;

$$I(q) = \int_0^\infty R^3{}_g(z) \exp(-R_g(z)^2 q^2 / 3) \exp(-\mu z / \sin\theta_i)$$

$$* \exp(-\mu z / \sin(2\theta_G - \theta_i)) dz \qquad (3)$$

The term Rg^3 in (3) comes from the fact that the scattering intensity is proportional to the square of the volume, whereas the number of GP zone is inversely proportional to the volume. The angle of exit, θf in (3) is replaced by an angle in the Guinier region, θ_G. This replacement causes a peaked distribution of the Guinier radius in Fig.3. As easily recognized from (3), the
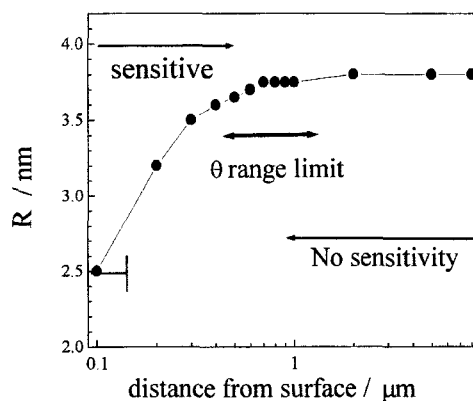
Fig.5 A reconstructed depth distribution of the average radius using equation (3) and the experimental data shown in Fig. 3. Since the Guinier radius for the lowest angle may be the average over some tens of nanometers due to surface undulation during quench, the point is shown with a lateral error bar. For the region shown as 'no sensitivity', the radius should converge to the bulk radius, but can not be determined by GI-SAXS.

limit of the angle of incidence is, and therefore, the penetration depth is strongly dependent on the size of the precipitates. In the following, we discuss the limitation of GI-SAXS on the application to a near surface precipitation structure.

4.2 Measurement conditions for the Guinier plot

When a penetration depth is drawn as a function of the incident angle, the graph suggests that the penetration depth increases monotonically with the angle. However, as suggested by (3), when we are interested in measuring a scattering intensity profile from precipitates, we need to analyze the intensity at an appropriate magnitude of the scattering vector. Since present analysis on the precipitate size is based on the Guinier approximation, the appropriate scattering vector, or the angle region, should be the Guinier region. In general, the Guinier approximation should be made at as smaller angle as possible. However, most of the precipitation structures examined in the metallurgical studies are not suitable for this general guideline, since the volume fraction of precipitates is often large enough so that the effect of interparticle interference destroys the form factor of individual precipitate at ideally small angle for the Guinier approximation.

A Guinier plot of a model calculation for a scattering intensity is shown in Fig. 6. The intensity was calculated for a system with spherical particles with a size distribution, and the scattering vector, q, is normalized by the average radius, R. A size distribution was introduced simply to avoid strong oscillation from the form factor of monodisperse spheres. The filled squares correspond to the calculated form factor, and the open circles corresponds to the from factor multiplied by the structure factor, i.e., the interparticle interference. The latter is regarded as a model of a measured small angle scattering intensity for a sample with finite volume fraction. The figure suggests that we may use the intermediate angle region, denoted by B, for the Guinier approximation. Then, we may use the condition, qR=2 for the angle of Guinier approximation, θ_G, for further discussion. Figure 6 strongly suggests that the Guinier
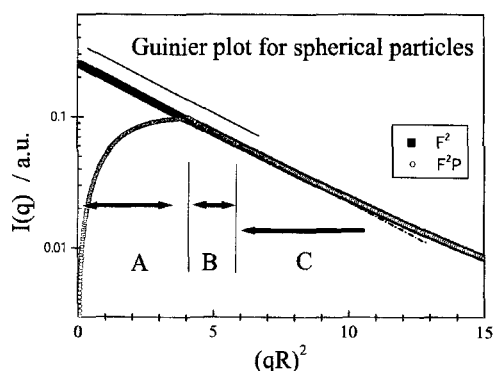
Fig. 6. Guinier plot for a model scattering intensity calculated for spherical particles with a size distribution, and with average interparticle distance, L=3R. The figure shows that the region A, an ideal angle region for Guinier approximation for the form factor, can not be used for the data analysis, and the region B may be used with a fair quality, region C with only poor quality.

approximation should be made at a constant and an appropriate value of qR, to keep the quality of the analysis. Therefore, concerning the quality of the Guinier plot, the model calculation suggests that the plot should be made with the condition of qR=constant for each plot.

However, considering the present experimental condition that the average radius changes with the depth, z, the appropriate method for Guinier approximation may not be the same as the above. Figure 7 gives the effective penetration depth calculated from (3) with a condition qR=2 for several size of precipitates. Since the calculation deals with a simple absorption, the value for the angle less or near the critical angle is irrelevant. For larger angles, it is clearly seen that,

1) The penetration depth gives a maximum at θ_G, and the depth is about 0.3 μm for a particle with R=3 nm.

2) When one changes the angle for the Guinier plot to adopt the change in the Guinier radius, it simultaneously change the effective penetration depth.

In the present analysis, we took the condition,

θ_G=constant, instead of qR=constant.
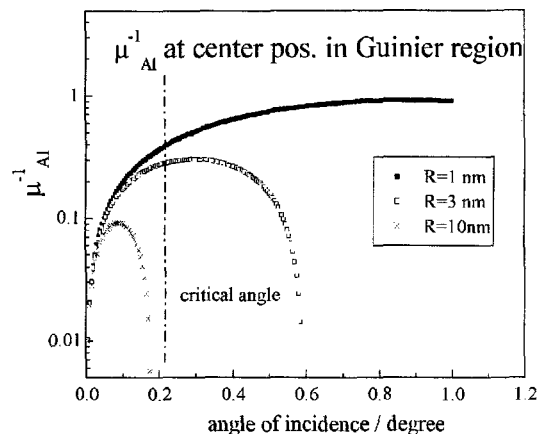
Fig. 7 Effective penetration depth for several sizes of precipitates. Larger precipitates with R=10 nm can not be evaluated within kinematical scheme.

4.3 Comparison with computer simulations

A kinematical analysis of the experimental GI-SAXS data leads to a conclusion that the average radius is smaller near the surface. Since the experiment was carried out with two step aging, with first step of quenching to room temperature under vacancy depletion, and with the second one at annealing temperature with uniform vacancy, a Monte Carlo simulation was made to check if the first step of aging lead to a smaller average radius during the second aging step. When we calculated the cluster size distribution at second aging at 0.6Tc for 10^3 MCS after the first aging at 0.55Tc for 10^3 MCS, a clear region with smaller cluster size was observed near the surface. Therefore, we may conclude that the vacancy depletion at the first step of annealing leads to a smaller zone radius even after the second annealing.

5. CONCLUSION

GI-SAXS measurements of an aged Al-Ag sample were made for several angle of incidence. Depth profile of the GP zone radius was calculated within kinematical approximation. Several limitations imposed on the application of GI-SAXS to surface precipitation structure has been discussed.

References
[1] P.N.T. Unwin, G.W. Lorimer and R.B. Nicholson, *Acta Metall.*, **17**,1363(1969).
[2] A.K.Vasudevan and R.D. Doherthy *Acta Metall.*, **35**,1193(1987).
[3] V. Gerold, "Small-angle scattering", Ed. by Brumberger, Gordon and Breach, N.Y.(1967) p277-317.
[4] A. Naudon, "Modern Aspects of Small-angle Scattering", Ed. by H.Brumberger, Kluwer Academic, Dordrecht(1995) p.181-203.